RSC Advances

PAPER

View Article Online
View Journal | View Issue

Cite this: *RSC Adv.*, 2017, **7**, 45615

Bifunctional electro-catalytic performances of $CoWO_4$ nanocubes for water redox reactions (OER/ORR)

Saad M. AlShehri,[a] Jahangeer Ahmed,*[a] Tansir Ahamad,[a] Prabhakarn Arunachalam,[a] Tokeer Ahmad[b] and Aslam Khan[c]

Received 30th June 2017
Accepted 18th September 2017

DOI: 10.1039/c7ra07256b

rsc.li/rsc-advances

In this paper, we report the synthesis of cube shaped nanoparticles of $CoWO_4$ (~30 nm) by molten salts and their bifunctional electro-catalytic activities in water redox reactions for oxygen evolution and oxygen reduction reactions (OER and ORR). Bifunctional performances of $CoWO_4$ nano-cubes are explored for water electrolysis in an alkaline medium (1.0 M KOH) *vs.* reversible hydrogen electrode (RHE) under various atmospheres (N_2, air and O_2). Low overpotential (η_{10} = 0.45 V) of $CoWO_4$ nano-cubes is accomplished at the current density of 10 mA cm^{-2}. Tafel polarization curves (potential *vs.* log current density) reveal relatively lower slope values for OER (~82 mV dec^{-1}) and ORR (~68 mV dec^{-1}) compared to previous reports. Stability test of electrode materials has been performed using chrono-amperometry (CA) at fixed potential for 500 seconds. Kinetics and mobility of electrons have also been studied during the water redox reactions. Stable nature and enhanced bifunctional electro-catalytic performances of earth abundant $CoWO_4$ electrodes could be used as the replacement of expensive electroactive noble electrode materials (Pt, Ir, Ru *etc.*) for water electrolysis (OER and ORR) in near future.

Introduction

Development of new renewable energy based technology is the current challenge to the researcher due to high global energy consumption and crisis of fossil fuel. Therefore, it encourages us to build up reliable substitutes for non-sustainable energy sources (*e.g.* oil, coal, natural gases *etc.*) on a large scale with low cost of production. Electrolysis of water is the most proficient and ecofriendly process to provide the clean, renewable and sustainable energy resources like H_2–O_2 fuel cells,[1] metal–air batteries,[2,3] and metal–oxygen batteries.[4,5] Electrolysis of water to evolve the gases like H_2 or O_2 is significant to provide sustainable energy through various devices. H_2 can be used as a fuel in fuel cells by converting the chemical energy into electrical energy. H_2 reacts with O_2 to produce electric current in a fuel cell. O_2 can also be used in fuel cells to generate the power by the combustion of the fuels. Precious metals (*e.g.* Pt, Ir, Rh, Ru *etc.*) or their oxides were widely used as the electroactive electrode materials in water electrolysis process for gas evolution and reduction reactions[6–11] but their uses as commercially are limited due to very high cost. Cobalt and tungsten are the earth abundant elements and $CoWO_4$ electrode materials could be efficient in water electrolysis reaction compared to noble electrode materials. Therefore, our main concern is to fabricate the low cost electrode materials with efficient electro-catalytic activity and zero tolerance of environmental pollutions. Current work emphases the bi-functionality and stability of $CoWO_4$ electrode materials for clean and sustainable energy *via* electrochemical water splitting in alkaline medium. OER and ORR are the significant reactions of water electrolysis to develop the required cost effective anode and cathode materials, respectively, with high stability, low Tafel slope, and low overpotential for the long term energy applications.

Cobalt based nanocrystalline materials (*e.g.* oxides,[12–14] hydroxides,[15] phosphates,[16–18] sulfides,[19,20] mixed metals[21,22] *etc.*) were considered as the effective water oxidation electrocatalysts. In recent years, metal–tungstate (MWO_4; M = Co, Ni, Mn *etc.*) nanostructured materials have attracted much attention as substantial electro-catalysts for the electrolysis of water.[23–26] Surface dependent water electrolysis on $CoWO_4$ (010 surface) were examined by controlling the high overpotentials (~0.97 V for OER) to stabilize the oxygen radicals during OER.[26] Tafel slopes of amorphous and crystalline $CoWO_4$ materials were reported ~60 mV per decade and ~110 mV per decade, respectively, for water oxidation *versus* normal hydrogen electrode (NHE).[25] Metal tungstate (MWO_4; M = Co, Ni) nanoparticles have also shown significance in supercapacitors applications.[27] $CoWO_4$ nanoparticles were also used as the electro-catalysts for the reduction of *p*-nitrophenol,[28] non-enzymatic glucose sensors,[29]

[a]*Department of Chemistry, College of Science, King Saud University, Riyadh 11451, Kingdom of Saudi Arabia. E-mail: jahmed@ksu.edu.sa*

[b]*Nanochemistry Laboratory, Department of Chemistry, Jamia Millia Islamia, New Delhi 110025, India*

[c]*King Abdullah Institute for Nanotechnology, King Saud University, Riyadh 11451, Kingdom Saudi Arabia*

non-enzymatic H_2O_2 sensors.[30] $CoWO_4$ nanoparticles were also reported as the electro-catalysts for oxygen evolution reactions (OER) but from the best of our literature survey, oxygen reduction reactions (ORR) using $CoWO_4$ nano-catalysts are still missing. A series of delafossites nanostructured materials has been developed by Ahmed *et al.* for oxygen and hydrogen evolution reactions (OER and HER) from the electrochemical water splitting reaction in alkaline medium.[31–33] Though, the present work covers water redox reaction (OER/ORR) over the surface of bifunctional $CoWO_4$ electro-catalysts in alkaline medium (1.0 M KOH) at room temperature. Moreover, we also report the synthesis of $CoWO_4$ nano-cubes from the molten salts process at 500 °C. In this process, molten salts function as the solvent like water; and excess of molten salts play the fundamental role in term of transferring of the sufficient amount of energy to the precursor materials to control the final products in nano-metric region. This is noteworthy that molten salt procedure is one of the most favorable, simple, eco-friendly, and less expensive method to synthesize the variety of nanostructured materials with uniform particles size. Phase purity, crystal structure, morphology and surface area of $CoWO_4$ nanocubes were investigated by FTIR, powder X-ray diffraction (PXRD), X-ray photoelectron spectroscopy (XPS), electron microscopy, and N_2 adsorption–desorption BET measurements. Bifunctional and stable electro-catalytic activities of $CoWO_4$ nanocubes for OER and ORR were investigated in details using CV, LSV, CA and Tafel polarization studies in alkaline medium *vs.* RHE.

Experimental

1 mol of $CoCl_2 \cdot 6H_2O$ (BDH, 98%), 1 mol of $Na_2WO_4 \cdot 2H_2O$ (BDH, 96%), 30 mol of $NaNO_3$ (Alfa Aesar, 98+%) and 30 mol of KNO_3 (Alfa Aesar, 99%) reagents were mixed together and ground an agate mortar pestle for half an hour to make the homogeneous mixture of molten salts. The resulting homogeneous mixture was placed in to the covered crucible and transferred to the high temperature furnace. The mixture was fired at 500 °C for 6 h in air. The grey colored powder was obtained and washed five times by de-ionized water and then dried in oven at 60 °C. The reaction temperature of 500 °C in the synthesis of materials was considered according to the reported phase diagram of the molten salts ($NaNO_3$ + KNO_3).[34] Note that so far no previous report is found in literature on molten salts synthesis of $CoWO_4$ nanocubes. Molten salts synthesis is very simple, cost effective, and environmental friendly procedure to prepare the single phase nanocrystalline materials with controlled shape and size by controlling the reaction parameters like nature of salts, molar concentration, temperature, rate of reactions *etc.*[9,35–37] Excess of molten salts (KNO_3 + $NaNO_3$) work as the solvent like H_2O and also play a significant role for transferring of energy to the precursor to control the shape and size of the nanostructured materials. The final product ($CoWO_4$ nanocubes) was initially characterized by powder X-ray diffraction (PXRD) to investigate the phase purity and crystal structure of the nanopowder. PXRD data of $CoWO_4$ nanocubes was recorded on X-ray diffractometer (Rigaku MiniFlex, Ni-filtered Cu-Kα radiation) consisting step size of 0.02° with scan speed of 1 s. FTIR data was recorded on a Bruker TENSOR 27 Spectrometer in the range of wavenumber from 400 to 4000 cm^{-1}. Field emission scanning electron microscope (FESEM, JEOL JSM-7600F) and high resolution transmission electron microscopic (HRTEM, JEOL JSM-2100F) studies were carried out to find the exact size and morphology of the final product. FESEM and HRTEM were operated at 5 kV and 200 kV respectively. Procedure to prepare the TEM specimen is reported elsewhere.[32] The surface area of $CoWO_4$ nanocubes was measured by the Brunauere–Emmett–Teller (BET) measurements using a V-Sorb 2800 Porosimetry Analyser (Gold APP Instruments, China).

Electro-catalytic tests were conducted by cyclic voltammetry (CV), linear sweep voltammetry (LSV) and Tafel measurements on computer controlled three electrode electrochemical work station (potentiostat/galvanostat, CHI 660E, China) electrochemical analyzer at 25 °C. In this study, Ag/AgCl is used as a reference electrode which is converted in to reversible hydrogen electrode (RHE) using the following the conversion scheme *i.e.* Nernst equation ($E_{(RHE)} = E_{(Ag/AgCl)}$ + 0.059 pH + 0.197 V) at 25 °C.[38] The slurry was prepared by the addition of 2.5 mg of catalysts to 0.5 ml of isopropanol with 0.1 ml of Nafion solution followed by the sonication for 10 minutes. One drop of slurry was placed on to the active surface of glassy carbon (GC) and then dried in oven at 50 °C. The loaded amount of $CoWO_4$ catalysts was maintained of 0.28 mg cm^{-2} on GC electrode for the electrolysis of water. The GC electrode (0.07 cm^2) and Pt-wire serve as the working electrode and counter electrode respectively. The electro-active surface area of electrode can be calculated using R–S equation.[39,40] Cyclic voltammetry (CV), linear sweep voltammetry (LSV) and Tafel experiments were carried out by applying the cathodic–anodic potential *versus* reference electrode in 1.0 M KOH electrolyte at room temperature in air, N_2, and O_2-saturated conditions for OER and ORR with the scan rate of 10 mV s^{-1}.

Rotating disc electrode was also used in LSV experiments with different rotations (*i.e.* 500, 1000, 1500, 2000, 2500 and 3000 rpm) for ORR in order to calculate the number of electrons involved in water redox reactions with the help of Koutecky–Levich (K–L) equation.[41,42] Chronoamperometry was also carried out to check the stability of electrode materials by applying the fixed potentials (1.7 V *vs.* RHE) for 500 seconds. Note that freshly prepared electrodes were used in each experiment.

Results and discussion

The crystallographic (powder X-ray diffraction) studies were carried out initially to identify the crystalline nature and phase purity of $CoWO_4$ nanocubes (Fig. 1a). Powder X-ray diffraction (PXRD) studies reveal high crystallinity of the nanomaterials. PXRD patterns perfectly match with JCPDS file (#15-0867) and can be indexed on the basis of monoclinic wolframite structure of $CoWO_4$. Present methodology is capable to synthesize the $CoWO_4$ nanocubes with high purity as shown no impure peaks detected (*e.g.* CoO, Co_2O_3, WO_3 *etc.*) in PXRD patterns. FTIR spectrum of $CoWO_4$ nanocubes is shown in Fig. 1b. The bands at ~3424 and ~1630 cm^{-1} resemble to the –OH group which could be arises due to the presence of moisture in atmospheric

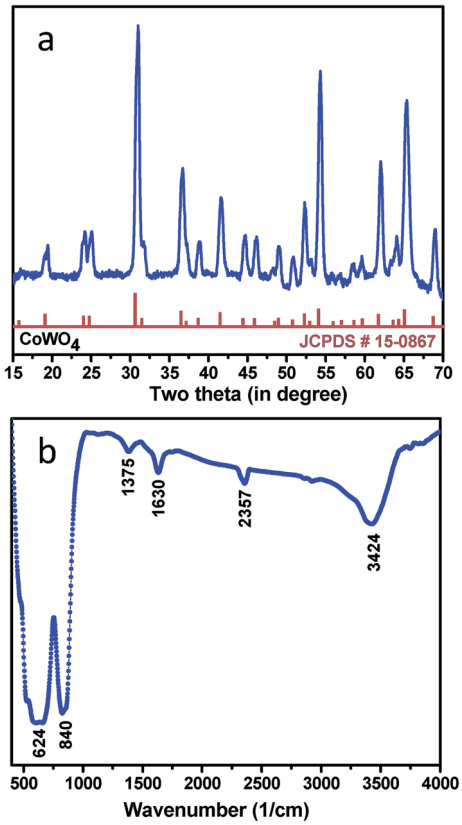

Fig. 1 (a) Powder X-ray diffraction patterns (PXRD), and (b) FTIR of $CoWO_4$ nanocubes.

conditions. The characteristics bands at ~624 (broad band from 690 to 580 cm^{-1}) and ~824 cm^{-1} are attributed to ν(Co–O)[43] and ν(W–O),[44] respectively, which confirm the formation of cobalt tungstate materials. XPS spectra of as-prepared $CoWO_4$ nanopowders were recorded and core level O 1s, W 4f and Co 2p spectra were observed as shown in Fig. 2a. Fig. 2b represents the local XPS region of Co 2p, contain two sets of doublets and shakeup satellites (abbreviated as "Sat."). The observed peaks at 780.89 and 796.63 eV could be assigned to Co $2p_{3/2}$ and Co $2p_{1/2}$, respectively.[45] The O 1s peaks were obtained at 529.21 and 529.86 eV as shown in Fig. 2c. It was also observed that during the calcination of the sample at high temperature in air the excess oxygen can be incorporated in the compound. The high-resolution spectrum of W 4f is shown in Fig. 2d, two XPS peaks were observed at 34.46 and 36.71 eV correspond to W $4f_{7/2}$ and $4f_{7/2}$ which indicate that W has a valence of +6 in the compound.[46]

Molten salts based synthesis leads to the formation of cubes shaped nanoparticles of $CoWO_4$ at 500 °C. The morphological characterization of the materials was investigated from FESEM and TEM studies. FESEM and TEM studies show the formation of cube shaped nanoparticles of $CoWO_4$ (Fig. 3a and b) and confirmed by the high resolution TEM studies with an average size of ~30 nm (Fig. 3c and d). A histogram of particle size distribution of $CoWO_4$ nanocubes is shown in Inset of Fig. 3a. A careful visualization of high magnification TEM studies of $CoWO_4$ nanocubes reveals that the nanocubes are formed from very tiny nanoparticles (Fig. 3c). The average size of these tiny particles was found to be ~1.0 nm. High resolution TEM studies of $CoWO_4$ nanocubes showed the crystalline nature of the materials as shown in Fig. 3d. The *d*-spacing of $CoWO_4$ nanocubes (~2.90 Å) was obtained from HRTEM which exactly match with the most intense line of X-ray diffraction patterns. This *d*-spacing value represents the most intense plane $\langle\bar{1}11\rangle$ of monoclinic crystal structure of $CoWO_4$ nanocubes. Synthesis of $CoWO_4$ nanoparticles (particle size from 30 to 200 nm) were also reported elsewhere using the co-precipitation[23,25,47] and hydrothermal methods.[28,29] Porous $CoWO_4$ nanofibers were reported by Sheng-Hui Liao *et al.* using the electrospinning method followed by firing at high temperature (625 °C).[30]

FESEM-EDAX (field emission scanning electron microscopy-energy dispersive X-ray spectroscopic) studies of $CoWO_4$ nanocubes were carried out for the elemental analysis. The atomic weight percent in the nanocubes was found to be nearly in equal ratio of Co and W (*i.e.* 1 : 1) as shown in Fig. 4a. The resulting composition is in accordance to the initial loaded composition. BET surface area of $CoWO_4$ nanocubes was examined from the N_2 adsorption–desorption isotherm (relative pressure (P/P^o) *vs.* adsorbed volume of N_2) as shown in Fig. 4b. The range of relative pressure (P/P^o) was used from 0.0 to 1.0. The BET surface area of $CoWO_4$ nanocubes (~13.5 $m^2\ g^{-1}$) is found to be quite similar to the other reports as the difference is quite small that likely varies batch to batch conditions.[23,25,28] All the properties (including physical, chemical, and biological) of the nanomaterials depend on the surface area per unit volume. High surface area of the materials could enhances the rate of reactions due to large number of reacting sites on to the surface of materials.

Electro-catalytic behavior of $CoWO_4$ nanocubes for water redox reactions (OER and ORR) was investigated from cyclic voltammetry (CV), linear sweep voltammetry (LSV) and Tafel measurements using 1.0 M KOH electrolyte *vs.* RHE with scan rate of 10 mV s^{-1} under various atmospheric condition (*e.g.* N_2, air and O_2-saturated). Fig. 5a represents the CV curves of $CoWO_4$ nanocubes in N_2 (black), air (red) and O_2-saturated (blue) for water redox reaction *i.e.* OER (anodic sweep) and ORR (cathodic sweep). CV curves of $CoWO_4$ nanocubes show that OER starts from low applied potential (1.54 V) *vs.* RHE. $CoWO_4$ nanocubes generate higher current in O_2-saturated atmosphere compared to air or N_2 atmosphere to OER as it was expected. The current density was found to be 15, 7.5, 7.5 mA cm^{-2} in O_2-saturated, air and N_2, respectively, at 1.75 V *vs.* RHE for evolution of oxygen. More importantly, CoWO4 nanocubes also show oxygen reduction reactions (ORR) in alkaline medium. From CV curves, we observed that the catalytic activity of $CoWO_4$ nanocubes for ORR reaction is higher in O_2-saturated system compared to air or N_2. The catalytic activity for ORR is also found to be better in air than N_2 during cathodic sweep as it was expected. The dissolved O_2 in 1.0 M KOH electrolyte could be removed by passing the nitrogen thoroughly. The onset potential for ORR is found to be ~0.70 V in O_2-saturated 1.0 M KOH against RHE. Previously, $CoWO_4$ nanoparticles were also used as the OER catalysts in alkaline medium against reference electrode (*e.g.* Hg/HgO or Ag/AgCl or RHE).[23,25,26] So far, $CoWO_4$ nanostructured materials

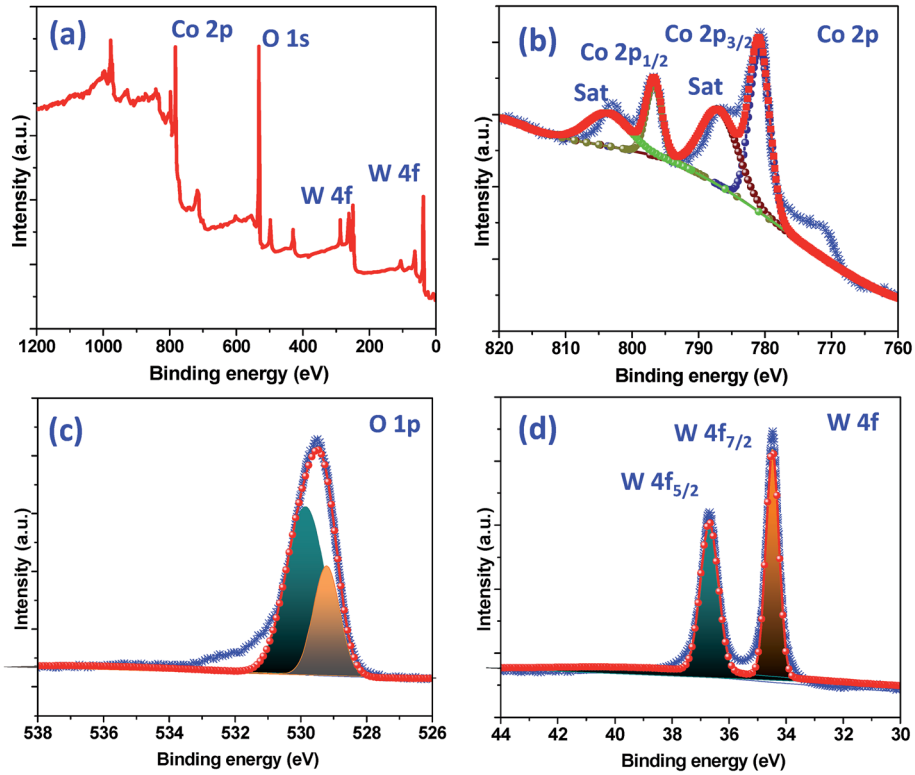

Fig. 2 XPS spectra of prepared $CoWO_4$ powers (a) survey (b) Co 2p (c) O 1s and (d) W 4f.

were reported as the electro-catalysts for OER only but our work demonstrate that $CoWO_4$ nanocubes have also shown the potential for both reactions, OER and ORR, in alkaline medium. However, $CoWO_4$ nanocubes show influential catalytic activity for the redox reaction of water to OER and ORR in alkaline medium *vs.* RHE. Noble metals (*e.g.* Ir, Pt, Ru *etc.*) and their

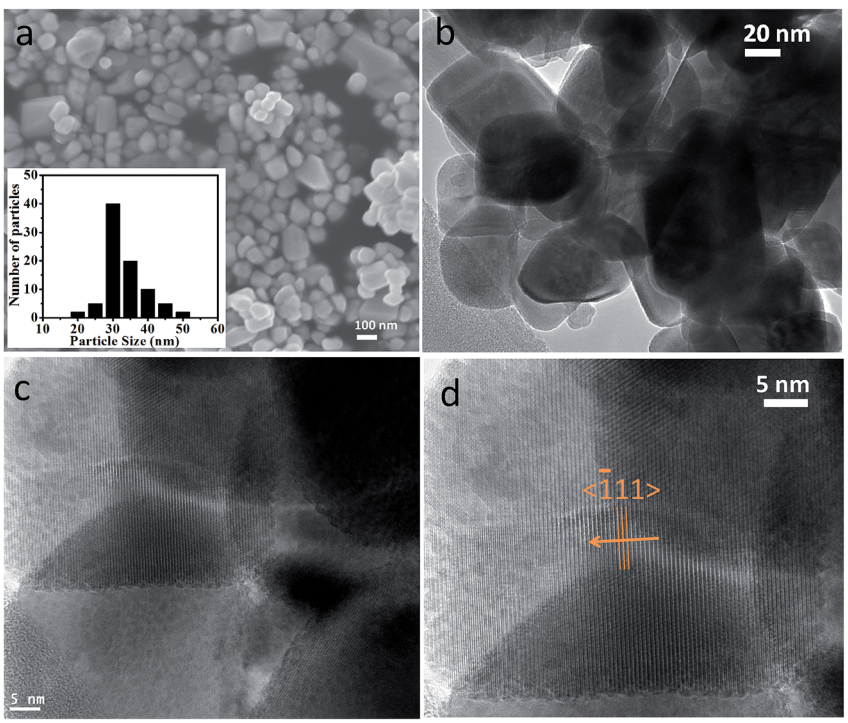

Fig. 3 (a) FESEM, (b) TEM, and (c, d) HRTEM micrographs of $CoWO_4$ nanocubes. Inset of (3a) shows a histogram of particle size distribution of $CoWO_4$ nanocubes.

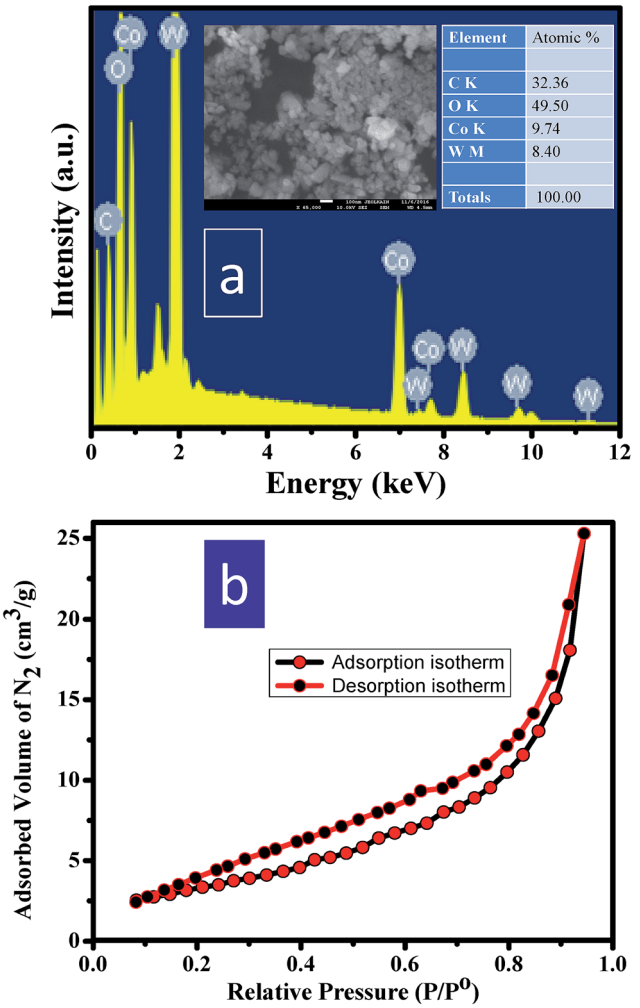

Fig. 4 (a) FESEM-EDAX, and (b) N_2 adsorption–desorption isotherm of $CoWO_4$ nanocubes.

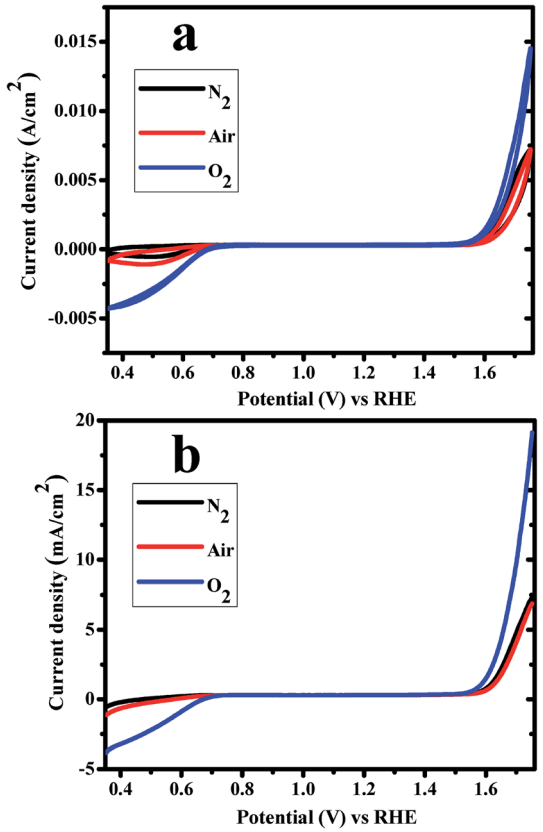

Fig. 5 (a) CV and (b) LSV curves of $CoWO_4$ nanocubes for water redox reactions in N_2, air and O_2 saturated 1.0 M KOH electrolyte *vs.* RHE with scan rate of 10 mV s^{-1}.

oxides have been used extensively as the electro-catalysts for water redox reactions since last one decade.[5] However, $CoWO_4$ nanocubes could work efficiently as the electro-catalysts for water oxidation reactions (OER and ORR) and can replace these expensive noble metals electro-catalysts for the better economy.

Linear sweep voltammetry (LSV) studies were also carried out to check the electro-catalytic activities of $CoWO_4$ nanocubes for water redox reaction (OER and ORR) in alkaline medium at the scan rate of 10 mV s^{-1} (Fig. 5b). The onset potentials of $CoWO_4$ nanocubes for OER and ORR were found to be ~1.54 V and ~0.70 V *vs.* RHE, respectively, which also support the results obtained from CV for bifunctional electro-catalytic activity. Moreover, LSV studies are also significant in order to estimate the overpotentials, Tafel values, reaction kinetics, and number of electrons involved during electrochemical reactions. The overpotential of $CoWO_4$ nanocubes (η_{10}) was estimated using the potential (V) at the current density of 10 mA cm^{-2} by the elimination of potential of water oxidation reaction. The overpotential (η_{10}) of $CoWO_4$ nanocubes was found to be 450 mV ± 5 for OER. The overpotentials were reported in the range from 350–970 mV for the water oxidation reactions over the surface of crystalline MWO_4 nanoparticles (M = Co, Ni).[23,25,26] Chen Ling *et al.* have explained that high overpotential could be ascribed due to the instability of resulted oxygen radicals during the water oxidation process.[26] This is noticeable that low overpotential of the catalysts plays a significant role to enhance the water oxidation reactions for OER, ORR, and HER.

The stability tests $CoWO_4$ nanocubes for OER were carried out by Charono-amperometric (CA) measurements (*i.e.* potentiostatic quantitative measurements) at the fixed potential (1.7 V) for 500 seconds in O_2-saturated 1.0 M KOH with controlled rotation (1000 rpm) of working electrode. CA is a potentio-static experiment *i.e.* true quantitative measurement of both stability and catalytic activity of the electrode materials in alkaline electrolyte. From the CA test, we observed that the resulting current densities are consistent with time. The electro-catalysts are stable and generating steady currents for the longer time as shown in Fig. 6. No current is generated without pasting the catalysts on the glassy carbon electrode. During the CA experiments, it is clearly observed that the water oxidation reaction stops immediately by switching off the potential and hence current drops to zero. Therefore, ternary oxides (*i.e.* $Co^{II}W^{VI}O_4$) are found to be stable electrode materials in alkaline medium for OER activities. The resulting current density of the materials with time directly proportional to the amount of gas evolved and consistency in the current density represents the stability of the electrode materials as well. The resulting current density of

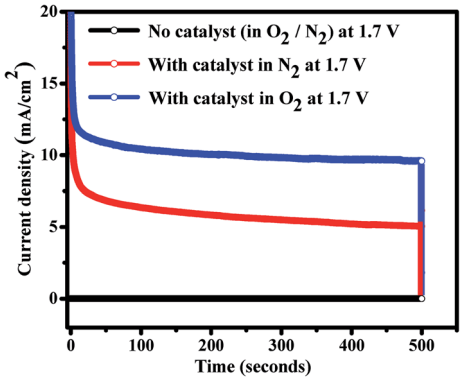

Fig. 6 Charono-amperometric (current *vs.* time) studies of $CoWO_4$ nanocubes for OER activity and stability check at 1.7 V.

$CoWO_4$ nanocubes (~10 mA cm^{-2} at 1.7 V) for OER is a function of both the surface area of the nanoparticle used and a combination of both faradaic and non-faradaic processes. The faradaic process results from charge being transferred across the electrode–electrolyte and is also governed by Faraday's law. In our case, four electrons were participated between the transition metal atoms (Co/W) and water molecules to evolve or reduced the O_2 gas. The non-faradaic process does not contribute to either ORR or OER as no charges are transferred and only induces the formation of the electrical double layer. The faradaic process is used in water redox reaction while both faradaic and double layer are present during the experiments. Therefore, the electrochemical experiments reveal that $CoWO_4$ is a stable electro-catalyst in water redox reactions. Previously, cobalt based heterogeneous catalysts have also been used as the bifunctional catalysts in water electrolysis using alkaline (1.0 M KOH), acidic or buffer electrolytic solutions.[48] The earth abundant electro-catalysts for long-term stability have always been considered as the potential catalysts for industrial applications in clean and renewable energy resources.

LSV experiments were again carried out for ORR in O_2-saturated 1.0 M KOH *versus* RHE using the rotating disk electrode (RDE) as the working electrode by applying the cathodic potential range at the scan rate of 10 mV s^{-1} (Fig. 7a). The rotation speed of RDE varies from 500 rpm to 3000 rpm for ORR experiments. This is evidently detected that the diffusion current densities of $CoWO_4$ nanocubes were increased significantly with the rotation speed due to the diffusion distance of O_2. Koutecky–Levich (K–L) equation was used to estimate the number of electrons and reaction kinetics involved in water redox reactions (Fig. 7b). Linear fitting curve between 1/current density (mA^{-1} cm^2) and $\omega^{-1/2}$ (rpm$^{-1/2}$) of the K–L plots reveals the 1st order kinetics of ORR in O_2-saturated alkaline medium. The number of transfer electrons (n) in water redox reaction was calculated and found to be in the range of 3.98–4.03 for the

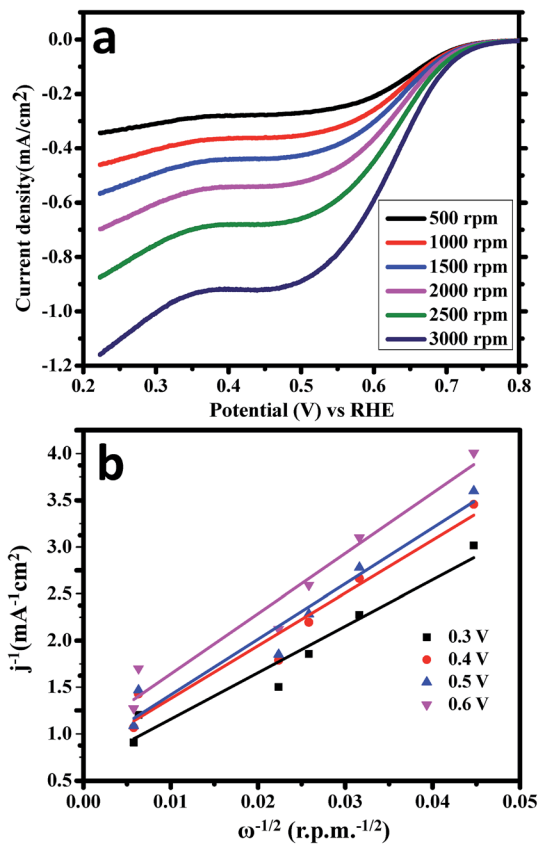

Fig. 7 (a) LSV measurements of $CoWO_4$ nanocubes for ORR with different rotation of RDE (500–3000 rpm). (b) K–L plots of $CoWO_4$ nanocubes for ORR in the potentials range from 0.30 V to 0.60 V *vs.* RHE.

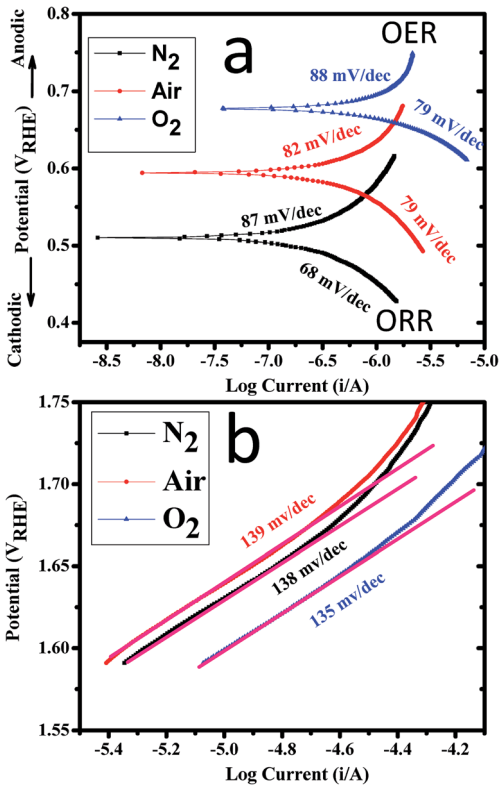

Fig. 8 Tafel polarization curves of $CoWO_4$ nanocubes at (a) low potential region and (b) high potential region for OER and ORR in 1.0 M KOH electrolyte with 10 mV s^{-1} scan rate.

Table 1 Comparison of present experimental details and results of as synthesized materials with literature

Electro-catalyst		$CoWO_4$ Nano-cubes	Strontium iron oxy-halides	Pt/C	IrO_2	IrO_2	Pt, Ir, Ru
Reference electrode		RHE	RHE	RHE	SHE	NHE	RHE
Electrolyte		1.0 M KOH	1.0 M KOH	2.0 M KOH	1.0 M $HClO_4$	1.0 N H_2SO_4	0.1 M $HClO_4$
Loaded amount (mg cm^{-2})		0.28	0.56	0.3	0.35	0.3	—
Scan rate (mV s^{-1})		10	50	5	10–500	1	50–500
Current density (mA cm^{-2})		15 at 1.7 V	10 at 1.7 V	6 at 1.7 V	2 at 1.5 V	15 at 1.8 V	0.5 at 1.2 V
Over-potential (mV)		450	350–970	—	450	—	—
Rotation speed of RDE (rpm)		500–3000	500–2000	400–1600	No RDE used	No RDE used	1600
Tafel slopes (mV dec^{-1})	OER	82	72–100	—	40–120	70–100	40–210
	ORR	62	87–98	65	—	—	—
Reference number		Current work	50	12	55	54	11

potential range from 0.30–0.60 V, which indicates that it favors a $4e^-$ oxygen reduction process as shown in Fig. 6b, close to the reported value of 4.00 of $NiCo_2O_4$/C and commercial Pt/C.[49]

Tafel polarization curves of $CoWO_4$ nanocubes for the OER and ORR activities are shown in Fig. 8 at low and high potential region. Fig. 8a shows the Tafel polarization curves of $CoWO_4$ nanocubes for the OER and ORR activities at low potential region. The observed values of Tafel slopes of $CoWO_4$ nanocubes were found to be ~87 mV per decade (in N_2), ~82 mV per decade (in air) and ~88 mV per decade for OER while Tafel values were found to be ~68 mV per decade (in N_2), ~79 mV per decade (in air), and ~79 mV per decade (in O_2) for ORR as shown in Fig. 8a. Recently, SrFe-oxy-halides were used as the electro-catalysts for water splitting (OER and ORR) in 1.0 M KOH against RHE and Tafel values were reported in the range from 72–100 mV dec^{-1} for OER and from 87–98 mV dec^{-1} for ORR.[50]

Fig. 8b shows the Tafel polarization curves of $CoWO_4$ nanocubes at high potential regions for the OER activity. Tafel slope values were found to be ~138 mV per decade (in N_2), ~139 mV per decade (in air), and ~130 mV per decade (in O_2) for OER activity at high potential region. The experimental error in the resulted Tafel slopes could be ±5. Tafel polarization studies are used to explain the reaction kinetics of water redox process depending on the size and surface area of the nanomaterials.[11] The linear fitting of the curves also shown the first order kinetics of the water oxidation reactions for OER and the value of *R*-squared (*i.e.* coefficient of determination) was found to be ~98.8% (Fig. 7c). This is noticeable that the R^2 values were found to be consistent in N_2, air and O_2. Based on the kinetics analysis on the steady state polarization curve (potential–current curve) for the OER mechanism is reported elsewhere.[51,52]

Tafel slope values were also reported in two different regions (low and high potential region) for oxygen evolution reaction (OER) using IrO_2–Ta_2O_5 electrodes in acidic medium. These slope values were reported of ~60 mV dec^{-1} and 130 mV dec^{-1} in the low potential region and high potential region, respectively, using saturated calomel electrode (SCE) as the ref. 52. Previously, Tafel slopes of crystalline $CoWO_4$ were also reported of ~110 mV dec^{-1} in O_2-saturated 0.2 M Na_2WO_4 electrolyte (pH = 6–8) using normal hydrogen electrode (NHE) as the ref. 25. Tafel values of cobalt based materials (*e.g.* CoMnP, $CoMnO_2$, Co_2P) were also accounted in the range from 61 mV dec^{-1} to 128 mV dec^{-1} in 1.0 M KOH against RHE which closely match with our results for OER.[53] Moreover, Tafel values of precious noble metals (*e.g.* Ru, Ir, Pt) and noble metals oxides (*e.g.* RuO_2, IrO_2 *etc.*) were reported in literature from 70–120 mV dec^{-1} and 44–210 mV dec^{-1}, respectively, for OER *via* water oxidation reactions.[11,51,54–56] This is noteworthy that as prepared materials show efficient catalytic activities to the OER and ORR by the electro-catalytic water redox reactions. The effective electrocatalysts for water redox reactions could lower the overpotential and Tafel slope values to sustain the high current and stability to enhance the efficiency due to loss of low energy during the electrochemical reactions. Table 1 shows the comparison of the experiments and results of current electro-catalytic activities (OER/ORR) of $CoWO_4$ nano-cubes with earlier reports.

Conclusions

$CoWO_4$ nanocubes were synthesized successfully from the molten salt process at 500 °C. Herein, these nanocubes are reported as the effective bifunctional and stable electrode materials for the water redox reactions (OER and ORR) in alkaline medium *vs.* RHE. K–L plot confirms that 4-electron system has been taking part in the redox reactions. Low overpotential, low Tafel slope values and high stability of $CoWO_4$ nanocubes demonstrated the low consumption of energy during the electrolysis of water. Therefore, the as synthesized catalyst ($CoWO_4$) consist the earth abundant elements that could have a significance impact over other electro-active precious catalysts (*e.g.* Pt, Au, Ir *etc.*) in the electrochemical energy conversion process.

Conflicts of interest

There are no conflicts to declare.

Acknowledgements

The authors extend their sincere appreciation to the Deanship of Scientific Research at King Saud University for funding this Research Group (RG-1435-007).

References

1 J. Vondrák, B. Klápště, J. Velická, M. Sedlaříková and R. Černý, *J. Solid State Electrochem.*, 2003, **8**, 44–47.
2 X. Zhang, X.-G. Wang, Z. Xie and Z. Zhou, *Green Energy & Environment*, 2016, **1**, 4–17.
3 Z.-L. Wang, D. Xu, J.-J. Xu and X.-B. Zhang, *Chem. Soc. Rev.*, 2014, **43**, 7746–7786.
4 I. Landa-Medrano, C. Li, N. Ortiz-Vitoriano, I. Ruiz de Larramendi, J. Carrasco and T. Rojo, *J. Phys. Chem. Lett.*, 2016, **7**, 1161–1166.
5 S. Xu, S. Lau and L. A. Archer, *Inorg. Chem. Front.*, 2015, **2**, 1070–1079.
6 C. Gutsche, C. J. Moeller, M. Knipper, H. Borchert, J. Parisi and T. Plaggenborg, *J. Phys. Chem. C*, 2016, **120**, 1137–1146.
7 R. Kumar, S. Pasupathi, B. G. Pollet and K. Scott, *Electrochim. Acta*, 2013, **109**, 365–369.
8 K. Eid, H. Wang, V. Malgras, S. M. Alshehri, T. Ahamad, Y. Yamauchi and L. Wang, *J. Electroanal. Chem.*, 2016, **779**, 250–255.
9 J. Ahmed and Y. Mao, *Electrochim. Acta*, 2016, **212**, 686–693.
10 S. Siracusano, V. Baglio, A. Stassi, R. Ornelas, V. Antonucci and A. S. Aricò, *Int. J. Hydrogen Energy*, 2011, **36**, 7822–7831.
11 T. Reier, M. Oezaslan and P. Strasser, *ACS Catal.*, 2012, **2**, 1765–1772.
12 K. Kumar, C. Canaff, J. Rousseau, S. Arrii-Clacens, T. W. Napporn, A. Habrioux and K. B. Kokoh, *J. Phys. Chem. C*, 2016, **120**, 7949–7958.
13 P. W. Menezes, A. Indra, D. González-Flores, N. R. Sahraie, I. Zaharieva, M. Schwarze, P. Strasser, H. Dau and M. Driess, *ACS Catal.*, 2015, **5**, 2017–2027.
14 F. Jiao and H. Frei, *Angew. Chem., Int. Ed.*, 2009, **48**, 1841–1844.
15 M. A. Ghanem, A. M. Al-Mayouf, P. Arunachalam and T. Abiti, *Electrochim. Acta*, 2016, **207**, 177–186.
16 Z.-G. Zhao, J. Zhang, Y. Yuan, H. Lv, Y. Tian, D. Wu and Q.-W. Li, *Sci. Rep.*, 2013, **3**, 2263.
17 Y. Zhan, S. Yang, M. Lu, Z. Liu and J. Y. Lee, *Electrochim. Acta*, 2017, **227**, 310–316.
18 M. W. Kanan and D. G. Nocera, *Science*, 2008, **321**, 1072–1075.
19 P. Ganesan, M. Prabu, J. Sanetuntikul and S. Shanmugam, *ACS Catal.*, 2015, **5**, 3625–3637.
20 Z. Luo, C. Tan, X. Zhang, J. Chen, X. Cao, B. Li, Y. Zong, L. Huang, X. Huang, L. Wang, W. Huang and H. Zhang, *Small*, 2016, **12**, 5920–5926.
21 J. Ahmed, B. Kumar, A. M. Mugweru, P. Trinh, K. V. Ramanujachary, S. E. Lofland, Govind and A. K. Ganguli, *J. Phys. Chem. C*, 2010, **114**, 18779–18784.
22 J. Ahmed, A. Ganguly, S. Saha, G. Gupta, P. Trinh, A. M. Mugweru, S. E. Lofland, K. V. Ramanujachary and A. K. Ganguli, *J. Phys. Chem. C*, 2011, **115**, 14526–14533.
23 V. K. V. P. Srirapu, A. Kumar, P. Srivastava, R. N. Singh and A. S. K. Sinha, *Electrochim. Acta*, 2016, **209**, 75–84.
24 B. Zhang, X. Zheng, O. Voznyy, R. Comin, M. Bajdich, M. García-Melchor, L. Han, J. Xu, M. Liu, L. Zheng, F. P. García de Arquer, C. T. Dinh, F. Fan, M. Yuan, E. Yassitepe, N. Chen, T. Regier, P. Liu, Y. Li, P. De Luna, A. Janmohamed, H. L. Xin, H. Yang, A. Vojvodic and E. H. Sargent, *Science*, 2016, **352**, 333–337.
25 H. Jia, J. Stark, L. Q. Zhou, C. Ling, T. Sekito and Z. Markin, *RSC Adv.*, 2012, **2**, 10874–10881.
26 C. Ling, L. Q. Zhou and H. Jia, *RSC Adv.*, 2014, **4**, 24692–24697.
27 G. He, J. Li, W. Li, B. Li, N. Noor, K. Xu, J. Hu and I. P. Parkin, *J. Mater. Chem. A*, 2015, **3**, 14272–14278.
28 L. Pan, L. Li and Y. Chen, *J. Sol-Gel Sci. Technol.*, 2013, **66**, 330–336.
29 M. Sivakumar, R. Madhu, S.-M. Chen, V. Veeramani, A. Manikandan, W. H. Hung, N. Miyamoto and Y.-L. Chueh, *J. Phys. Chem. C*, 2016, **120**, 17024–17028.
30 S.-H. Liao, S.-Y. Lu, S.-J. Bao, Y.-N. Yu and L. Yu, *ChemElectroChem*, 2015, **2**, 2061–2070.
31 J. Ahmed and Y. Mao, *J. Solid State Chem.*, 2016, **242**, 77–85.
32 J. Ahmed, V. V. Poltavets, J. Prakash, S. M. Alshehri and T. Ahamad, *J. Alloys Compd.*, 2016, **688**, 1157–1161.
33 J. Ahmed and Y. Mao, in *Nanomaterials for Sustainable Energy*, American Chemical Society, 2015, vol. 1213, ch. 4, pp. 57–72.
34 C. M. Kramer and C. J. Wilson, *Thermochim. Acta*, 1980, **42**, 253–264.
35 L. Li, J. Deng, J. Chen and X. Xing, *Chem. Sci.*, 2016, **7**, 855–865.
36 Y. Mao, T.-J. Park, F. Zhang, H. Zhou and S. S. Wong, *Small*, 2007, **3**, 1122–1139.
37 H. Zhou, Y. Mao and S. S. Wong, *J. Mater. Chem.*, 2007, **17**, 1707–1713.
38 S. J. A. Moniz, J. Zhu and J. Tang, *Adv. Energy Mater.*, 2014, **4**, 1301590.
39 A. A. A. Aljabali, J. E. Barclay, J. N. Butt, G. P. Lomonossoff and D. J. Evans, *Dalton Trans.*, 2010, **39**, 7569–7574.
40 I. Taurino, S. Carrara, M. Giorcelli, A. Tagliaferro and G. De Micheli, *Surf. Sci.*, 2012, **606**, 156–160.
41 Z. Wu, W. Li, Y. Xia, P. Webley and D. Zhao, *J. Mater. Chem.*, 2012, **22**, 8835–8845.
42 R. Zhou, Y. Zheng, M. Jaroniec and S.-Z. Qiao, *ACS Catal.*, 2016, **6**, 4720–4728.
43 M. Nidhin, K. J. Sreeram and B. U. Nair, *Chem. Eng. J.*, 2012, **185–186**, 352–357.
44 M. Mohamed Jaffer Sadiq and A. Samson Nesaraj, *J. Nanostruct. Chem.*, 2015, **5**, 45–54.
45 Y. Li, X. Li, J. Wang, Y. Jun and Z. Tang, *RSC Adv.*, 2017, **7**, 2919–2925.
46 X. Li, X. Li, Z. Li, J. Wang and J. Zhang, *Sens. Actuators, B*, 2017, **240**, 273–277.
47 F. Ahmadi, M. Rahimi-Nasrabadi, A. Fosooni and M. Daneshmand, *J. Mater. Sci.: Mater. Electron.*, 2016, **27**, 9514–9519.
48 J. Wang, W. Cui, Q. Liu, Z. Xing, A. M. Asiri and X. Sun, *Adv. Mater.*, 2016, **28**, 215–230.
49 J. Wang, Z. Wu, L. Han, R. Lin, H. L. Xin and D. Wang, *ChemCatChem*, 2016, **8**, 736–742.

50 M. A. Ghanem, P. Arunachalam, A. Almayouf and M. T. Weller, *J. Electrochem. Soc.*, 2016, **163**, H450–H458.
51 Y.-H. Fang and Z.-P. Liu, *J. Am. Chem. Soc.*, 2010, **132**, 18214–18222.
52 J.-M. Hu, J.-Q. Zhang and C.-N. Cao, *Int. J. Hydrogen Energy*, 2004, **29**, 791–797.
53 D. Li, H. Baydoun, C. N. Verani and S. L. Brock, *J. Am. Chem. Soc.*, 2016, **138**, 4006–4009.
54 K. Kadakia, M. K. Datta, O. I. Velikokhatnyi, P. H. Jampani and P. N. Kumta, *Int. J. Hydrogen Energy*, 2014, **39**, 664–674.
55 L. Ouattara, S. Fierro, O. Frey, M. Koudelka and C. Comninellis, *J. Appl. Electrochem.*, 2009, **39**, 1361–1367.
56 J. C. Cruz, V. Baglio, S. Siracusano, R. Ornelas, L. Ortiz-Frade, L. G. Arriaga, V. Antonucci and A. S. Aricò, *J. Nanoparticle Res.*, 2011, **13**, 1639–1646.